

PETROLOGIC AND THERMOBAROMETRIC ANALYSIS OF SILLIMANITE POD GNEISS OF FIVE POINTS GULCH, WET MOUNTAINS, COLORADO

GABRIEL ACEVEDO

University of Texas, El Paso

Sponser: Christopher Andronicos

INTRODUCTION

The Wet Mountains of Central Colorado are key to understanding the Proterozoic geologic evolution of the southwestern United States. Fundamental problems in deciphering the history of this region are to understand the pressure-temperature conditions of metamorphism and when these conditions were attained. This study focused on the first problem through investigation of mechanisms which led to the formation of sillimanite and using their petrogenesis to estimate the peak P-T conditions experienced by the gneisses exposed in the Arkansas River Canyon in the northern Wet Mountains (Figure 1). Sillimanite in these gneisses commonly forms large porphyroblastic masses up to eight centimeters in length ('pods'). This study has The findings will help to identify metamorphic field gradients present within the Wet Mountains.

Methods

Oriented samples used in this investigation were collected in the Arkansas River Canyon, and were thin sectioned for petrographic and microprobe analysis. A total of 36 samples have been used in this study and selected samples have been analyzed using the electron microprobe. Strain was quantified in five samples using the Fry method. Thin sections were scanned at a resolution of 600 DPI using

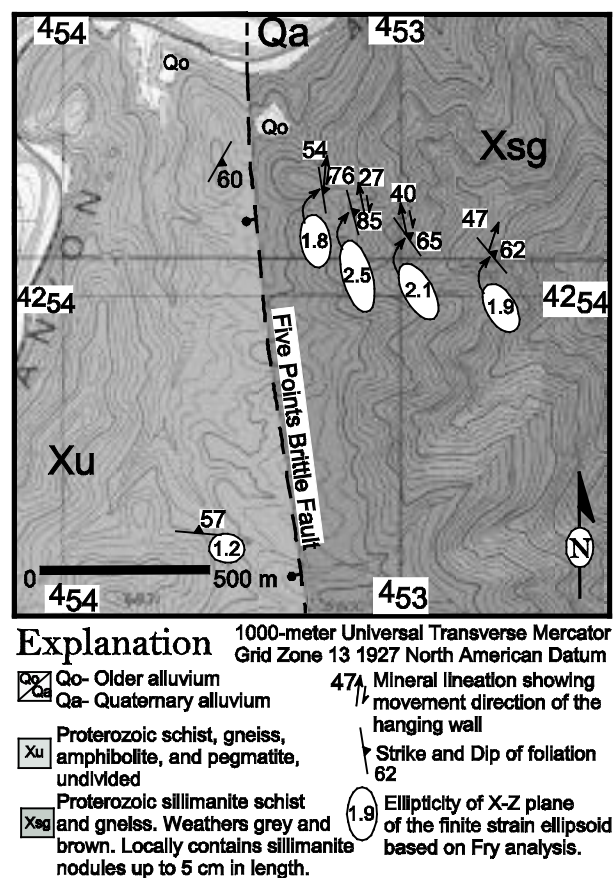


Figure 1. Simplified geologic map of study area.

a transparency adapter. Ilmenite grains were used as strain markers. Centers of at least 100 grains per thin section were chosen using the program GeoFry Plot maintained by Rod Holcombe

(<http://www.earthsciences.uq.edu.au/~rodh/software>).

Results

Grey-weathering sillimanite gneisses contain mineral assemblages which help constrain the peak metamorphic conditions. A typical grey assemblage is biotite-muscovite-sillimanite-plagioclase-K-feldspar-quartz-ilmenite. Biotite, muscovite and sillimanite are the main foliation-defining phases, whereas feldspars and quartz have more equigranular textures (Figure 2A).

Where sillimanite pods are present several different textures have been observed. The first are 1 to 2 cm elliptical nodules of sillimanite intergrown with muscovite (Figure 2B). Sillimanite within the nodules varies from fibrolitic to coarse needles of sillimanite. Within the nodules sillimanite appears to be randomly oriented whereas in the matrix sillimanite helps to define the foliation. Surrounding the nodules are abundant K-feldspar, quartz, biotite, and ilmenite.

Another commonly observed type of ‘pod’ is those with biotite rims, similar to those described by Foster (1990) and also described by Kerrick (1988). Foster and Kerrick both concluded that sillimanite nodules with rims of biotite form by fluid-driven diffusion of Fe and Mg. We focused our efforts on understanding the genesis of the sillimanite-muscovite nodules described above because of the relative chemical simplicity of the mineral assemblages in these rocks.

The association of sillimanite and K-feldspar suggests that “second sillimanite” metamorphic conditions were attained in these rocks. However, muscovite and quartz are abundant in all the samples examined in this study. This suggests that the metamorphic conditions were not well above the second sillimanite reaction boundary.

Chemically, muscovite in the samples can be divided into two types; muscovite within the pods and matrix muscovite. Microprobe analysis of matrix muscovite shows $X_K = .86$ (average of 40 analyses) where $X_K = K/(K+Na+Ca)$. Paragonite accounts for the

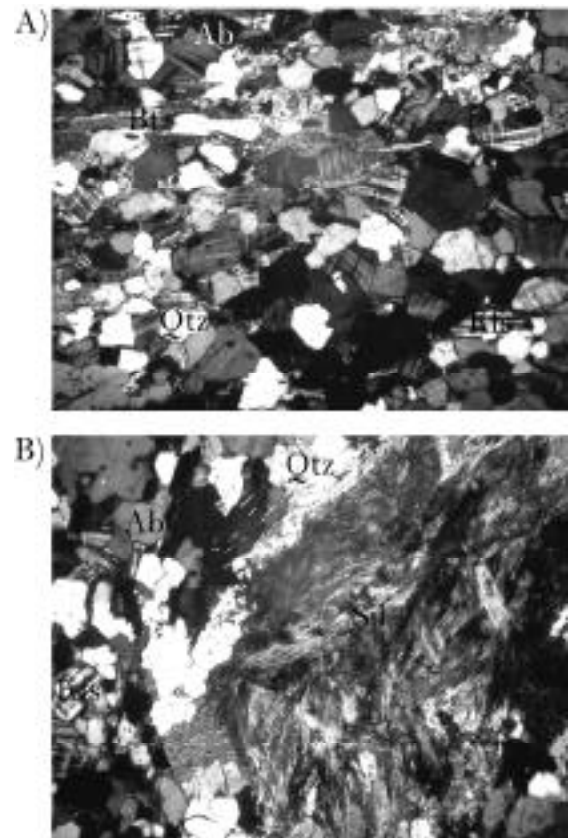
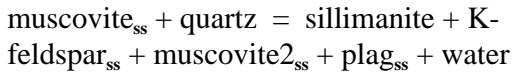


Figure 2. Photomicrographs of sillimanite pod gneiss. A) Photomicrograph showing typical matrix texture with biotite defining foliation, and quartz, plagioclase and K-feldspar with polygonal equigranular textures. B) Sillimanite pod showing mass of fine grained sillimanite replacing muscovite porphyroblast. Both fields of view, approximately 5 mm, cross polarized light.

remainder of the mica composition with Ca contents being lower than the detection limits of the microprobe analysis. In contrast, within the pods $X_K = .90$ (average of 10 analyses within the pods). Fewer analyses within the pods were obtained because the fine intergrowth of muscovite with sillimanite made obtaining points with pure muscovite difficult. However, our results do suggest that the composition of pod muscovite is distinct from that of the matrix with higher concentrations of Na occurring in the matrix muscovites. Plagioclase has complex zoning patterns. However, in general plagioclase rims have higher albite contents than the cores. These relationships suggest that the pod muscovites evolved from the matrix muscovites by a reaction of the form:



where ss denotes solid solution and muscovite2 is muscovite with different composition than the original phase. This suggests that the second sillimanite reaction evolved as a continuous reaction where the paragonite content of the mica decreased as the reaction progressed and the albite content of the plagioclase increased.

In order to constrain the P-T conditions of metamorphism in the rocks, the position of the sillimanite-forming reaction was calculated using the compositions of the phases determined from the sample. The mixing model of Chatterjee and Froese (1975) was used for the micas and the solution model of Fuhrman and Lindsey (1988) was used for feldspars. Quartz and sillimanite were treated as pure phases (Fig. 3). This reaction forms a line in P-T space stretching from approximately 570 °C and 2.5 kbar to 650 °C and 7 kbar within the sillimanite stability field using the Al_2SiO_5 triple point of Holdaway and Mukhopadhyay (1993). Using a value for the triple point at higher pressure and temperature (e.g. Pattison 1992) would further restrict the P-T interval of the reaction.

The compositions of biotite and muscovite were similar to those used by Hoisch (1989) to define an empirical thermometer based on tschermak exchange between biotite and muscovite. Applying this calibration to the mica compositions from the sillimanite pod gneiss results in a temperature of 620 °C at 3 kbar, and 690 °C at 7 kbar, consistent with second sillimanite conditions. An additional constraint on the P-T conditions in these gneisses is the lack of significant migmatitic textures indicating that conditions for melting were not attained within these gneisses. Assuming water saturation the phase relations and chemical data suggest P-T conditions between 3 and 6 kilobars and temperatures between 570 and 650 °C (grey region in figure 3). We are currently analyzing garnet-bearing samples which should help to refine our P-T estimates.

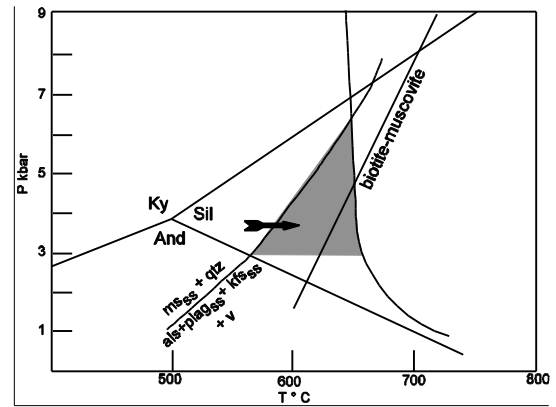


Figure 3. Pressure-temperature diagram for feldspathic sillimanite pod gneiss. Triple point is after Holdaway and Mukhopadhyay (1993). Granite melting curve is after Clemens and Wall (1981). Position of the Sillimanite-in reaction is calculated based on composition of coexisting plagioclase, K-feldspar and muscovite. Line labeled biotite-muscovite is calculated based on muscovite-biotite geothermometer of Hoisch (1989). Grey region is the estimated range of P-T conditions.

The intergrowths of sillimanite and muscovite within the sillimanite pods suggest transfer of alkalis from the pods to adjacent feldspars. We envision a mechanism where muscovite porphyroblasts begin to react to form sillimanite, albite and K-feldspar. Water evolved by the reaction leaches Na and K from the muscovite porphyroblasts and leaving behind Al_2O_3 rich selvages which form the sillimanite-muscovite pods. The depletion of the paragonite component of the pod muscovite suggest that Na was relatively more susceptible to removal from the pods than K. This preferential removal of paragonite from the mica is consistent with temperature increase as the reaction progressed. Our interpretations suggest that Al was relatively immobile during this process whereas Na, K and Si were relatively mobile, at least at the scale of the thin section.

STRUCTURE

The field area shows evidence for polyphase deformation. Two different shearing events were observed in the study area. The first is recorded by top-to-the-southwest reverse sense kinematic indicators developed within the sillimanite gneisses. Sillimanite pods are often deformed into asymmetric

porphyroclasts suggesting their development was either syn- or pre-kinematic. Fry analysis of samples recording reverse motion suggests ellipticities of the X-Z plane of the finite strain ellipsoid are fairly homogeneous for at least 500 m to the east of the Five Points brittle fault (Figure 1). Shear sense indicators which record sinistral northeast side down sense of motion were observed in amphibolites next to the Five Points brittle fault. Although direct overprinting relationships have not been observed between the reverse and sinistral deformation fabrics we favor an interpretation where reverse shearing predates sinistral shearing. If these interpretations are correct, then it is likely that development of the sillimanite pods occurred during Paleoproterozoic reverse shearing and crustal thickening.

CONCLUSIONS

The mineral assemblages and chemical data place constraints on the peak P-T conditions present during the formation of sillimanite pod gneiss within the Arkansas River Canyon. Our results suggest that peak temperatures were near 650 °C with pressures between 3 and 7 kbar. We favor the lower pressure end of this estimate based on the occurrence of andalusite and cordierite in nearby schists, although structural relationships preclude direct correlation between the rock packages. The formation of sillimanite pods appears to occur by the breakdown of mica through a continuous reaction where the paragonite component of the mica is depleted. The alkali elements K and Na are removed from the mica porphyroblast resulting in the production of a sillimanite-muscovite intergrowth.

The asymmetric shape of most of the pods indicates that metamorphism occurred concurrently with contractional deformation. Reverse shearing likely occurred during Paleoproterozoic crustal assembly. If these results hold up, they imply that Paleoproterozoic orogenesis resulted in upper amphibolite facies metamorphism in the Arkansas River Canyon of the Wet Mountains.

REFERENCES CITED

- Berman R. G. (1991) Thermobarometry using multiequilibrium calculations: a new technique with petrologic applications. *Canadian Mineralogist*, v. 29, p. 833-855.
- Berman, R.G. (1988) Internally-consistent thermodynamic data for stoichiometric minerals in the system Na₂O-K₂O-CaO-MgO-FeO-Fe₂O₃-Al₂O₃-SiO₂-TiO₂-H₂O-CO₂. *Journal of Petrology*, v. 29, p. 445-522.
- Chatterjee, N. D. & Froese E. F. (1975) A thermodynamic study of the pseudobinary join muscovite-paragonite in the system KAlSi₃O₈-NaAlSi₃O₈-Al₂O₃-SiO₂-H₂O. *Amer. Mineral.*, v. 60, p. 985-993.
- Clemens J.D., Wall, V.D. (1981) Origin and crystallization of some peraluminous (S-type) granitic magmas. *Can. Mineral*, v.19, p. 111-131.
- Foster, C.T. (1990) The role of biotite as a catalyst in reaction mechanisms that form fibrolite, *Geol. And Mineral. Assoc. of Canada*, 15, A40.
- Fuhrman, M. L. and Lindsley, D. H. (1988) Ternary-feldspar modeling and thermometry: *American Mineralogist*, v. 73, p. 201-216.
- Hoisch, D.T. (1989) A muscovite-biotite geothermometer. *American Mineralogist*, v. 74, p. 565-572.
- Holdaway, M.J., Mukhopadhyay, B (1993) A revelation of stability relations of andalusite; thermochemical data and phase diagram for aluminum silicates, v. 78, no. 1-2, p. 56-67
- Kerrick, D.M.(1988) Al₂SiO₅-bearing segregations in the Lepontine Alps, Switzerland: aluminum mobility in metapelites. *Geology*, v. 16, p. 636-640.
- Pattison, D.R.M (1992) Stability of andalusite and sillimanite and the Al₂SiO₅ triple point: constraints from the Ballachulish Aureole, Scotland. *Journal of Geology*, v.100, p. 423-446.
-